

Communication

Glass Transition in Crosslinked Nanocomposite Scaffolds of Gelatin/Chitosan/Hydroxyapatite

Karina N. Catalan ¹, Tomas P. Corrales ¹, Juan C. Forero ²  and Christian P. Romero ¹
and Cristian A. Acevedo ^{1,2,*}

¹ Departamento de Física, Universidad Técnica Federico Santa María, Valparaíso 2340000, Chile; kcatalans@gmail.com (K.N.C.); tomas.corrales@usm.cl (T.P.C.); christian.romero@usm.cl (C.P.R.)

² Centro de Biotecnología, Universidad Técnica Federico Santa María, Valparaíso 2340000, Chile; jcarlosforero@gmail.com

* Correspondence: cristian.acevedo@usm.cl; Tel.: +56-32-265-4730

Received: 21 March 2019; Accepted: 4 April 2019; Published: 9 April 2019



Abstract: The development of biopolymeric scaffolds crosslinked with nanoparticles is an emerging field. Gelatin/chitosan scaffolds are gaining interest in medical areas, e.g., bone tissue engineering, given their suitability for nano-hydroxyapatite incorporation. The glass transition temperature is a thermodynamic property of polymer scaffolds that changes with crosslinker or nanofiller concentration. Here, we report the experimental change in glass transition temperature of gelatin/chitosan scaffolds modified by hydroxyapatite nanoparticles and crosslinker concentration. Our results show synergic effects between nanoparticles and crosslinking, which leads to a non-linear behavior of the glass transition temperature. Furthermore, a theoretical model to predict glass transition is proposed. This model can be used as a mathematical tool for the design of future scaffolds used in bone tissue engineering.

Keywords: crosslinking; glass transition; nanoparticles; polymers; scaffolds

1. Introduction

In recent years, the development of biopolymeric scaffolds infiltrated with nanoparticles, i.e., nanocomposite scaffolds, have gained increasing interest for their applications in tissue engineering [1]. The benefits and toxic effects of nanoparticle addition within scaffolds have been extensively reported in literature, however, the thermodynamic aspects of their addition have not been studied in detail. Paul and Robeson reviewed the effects of nanofillers, such as clay-based nanocomposites, on the glass transition temperature (T_g) of a polymer matrix [2]. The glass transition temperature characterizes polymers, copolymers and biopolymers [3], as well as polymer-based composites. The T_g of nanocomposites with well-dispersed nanofillers can exhibit considerable deviations relative to the equivalent bulk polymer value. In some cases, T_g decreases as the interface between polymer and nanofiller produces free surfaces, and increases when the wetted interface yields attractive interactions [4]. Furthermore, biopolymer scaffolds used for tissue engineering must be crosslinked to avoid the dissolution in water. It is well known that the T_g of scaffolds increases significantly with crosslinking [5]. The change of glass transition temperature can be correlated with important aspects of the polymer structure, both micro- and nanostructure, which in turn affects the behavior of cells seeded on the tissue engineered scaffolds. Important microstructure properties and nanostructure characteristics can be explained and modeled by means of polymer theory, in particular their glass transition temperature (T_g) [6–8].

Biopolymer scaffolds made with mixtures of gelatin and chitosan are gaining interest in medical areas such as tissue engineering. Furthermore, gelatin/chitosan scaffolds are being used

as suitable materials for the incorporation of nanofillers, like hydroxyapatite, which is used in bone tissue engineering [9].

The understanding of glass transition behavior in crosslinked nanocomposite scaffolds is very important for the design of these materials. Glass transition studies have been used to design skin [10] and bone scaffolds [9], to understand the biodegradation of scaffolds [11] and to study the effect of sterilization using gamma radiation [12]. Reported values of T_g for bone tissue engineering scaffolds are in the range of 30–40 °C [9]. However, to the best of our knowledge, there are no readily available studies reporting the design of scaffolds as a function of both nanoparticle and crosslinker concentration simultaneously. In this work, we report changes in the glass transition temperature T_g of crosslinked scaffolds used for bone tissue engineering made of gelatin/chitosan/hydroxyapatite. We have analyzed these changes as a function of crosslinking and nanoparticle concentration, and propose a model that can be used as a scaffold design tool.

2. Materials and Methods

The crosslinked nanocomposite scaffolds were prepared using the freeze-drying method reported by Forero et al. [9], to prepare bone tissue engineering biomaterials. In brief, solutions of chitosan (0.5% w/v; 120 kDa; >85% deacetylated; Quitoquimica, Concepcion, Chile) and gelatin (0.25% w/v; type B; Merck, Darmstadt, Germany) were prepared at 50 °C in diluted acetic acid (100 mM). The solutions were modified by incorporation of hydroxyapatite nanoparticles (<200 nm; Sigma-Aldrich, St. Louis, MO, USA) and glutaraldehyde as crosslinker (Sigma-Aldrich, St. Louis, MO, USA). The solutions were poured onto Petri dishes, frozen at –20 °C and freeze-dried using the method described by the same authors [9].

To study the effects on T_g by nanoparticles and crosslinking, an experimental design was carried out. In this design two factors are included (full factorial design 3^2): Nanoparticle mass fraction (X) and crosslinker concentration (C). Each of these two parameters had three different levels. The levels for X were 0 (no nanoparticle added), 0.07 and 0.14. The levels for C were 0.02%, 0.06% and 0.10%. Statistical analyses were performed using the Modde software (Umetrics, Umea, Sweden).

The glass transition temperatures of the scaffolds were determined with a differential scanning calorimeter (Mettler Toledo, model DSC1, Greifensee, Switzerland), using the method previously described by Acevedo et al. [13].

3. Results and Discussion

3.1. Glass Transition Behavior

Glass transition is a key variable to design polymer scaffolds for tissue engineering. Given that T_g changes when the scaffold is crosslinked [8], irradiated [12] or biodegraded [11], it allows the detection of variations in the fabrication, sterilization or storage of the scaffold. Also, the T_g can be related with the nanostructure, which in turn, directly affects the cell behavior [6–8].

Figure 1 shows the results of the glass transition temperature. When no nanoparticles are added ($X = 0$), the T_g increases with the crosslinker concentration. This is a well-known phenomenon, that is due to the increase in the molecular weight of the polymer and can be described using the empirical Flory–Fox Equation [14]. However, when nanoparticles are used ($X = 0.07$ and $X = 0.14$), T_g decreases as shown in Figure 1. It has been previously informed in nanocomposites with dispersed nanofillers [12–14], that T_g can increase or decrease depending of the interaction that occurs within the material.

In Figure 2 we show the results of the experiment design analysis. Figure 2a shows that the effects of C and X on T_g are non-linear and that there are possible synergic effects between them. In Figure 2b we show that there is a nanoparticle-crosslinker interaction (CX) and a quadratic dependence on X . The estimation of the glass transition can be expressed with the equation $T_g(C, X) = k_1 + k_2CX + k_3X^2$ (where k_i are empirical parameters). Given that this model is empirical, it cannot be easily extrapolated

to other systems. To further understand our experimental results, it is necessary to derive a theoretical model that can be extended to different scaffolds. This will enable a description of the interactions between nanoparticles X and crosslinks C , as well as the quadratic dependence on X .

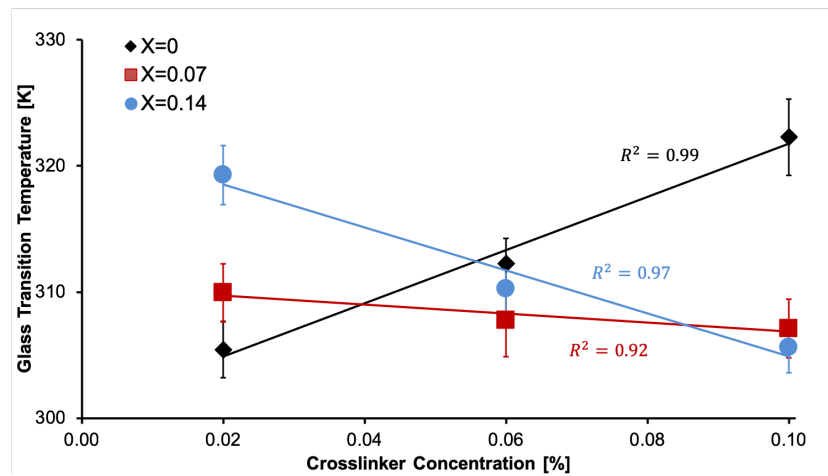


Figure 1. Experimental data of T_g in crosslinked nanocomposite scaffolds. Three mass fractions of nanoparticles were measured: $X = 0$, $X = 0.07$ and $X = 0.14$.

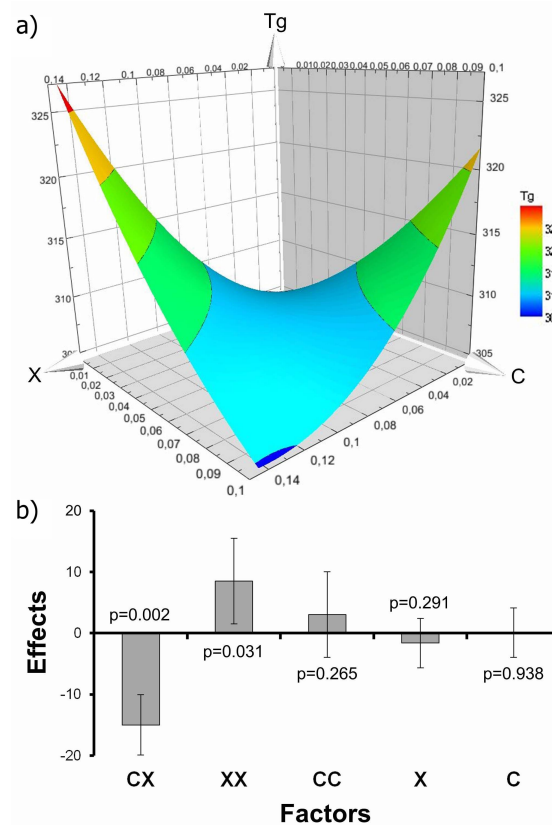


Figure 2. Results of the experimental design analysis for glass transition. (a) Surface plot for T_g as a function of C and X . (b) Effects plots (with p -values and error bars 95%) for T_g .

3.2. Theoretical Modelling

There are several mathematical models to study T_g in polymeric systems, e.g., thin films [15–18] and nanocomposites [19–21], but to the best of our knowledge, there are no available models to study T_g in scaffolds as a function of both nanoparticle X and crosslinker concentration C .

The theoretical work was done to understand the change in T_g observed in the scaffolds. To do this, we start with the model proposed by Lee et al. [19]. This model relates the glass transition with nanoparticle amount. We have modified this model to include the interaction between crosslink and nanoparticles. It has been reported [20], that the glass state formation is a result of the system's loss of configurational entropy (S), which is given by the configurational entropies of the liquid (S_{liquid}) and glass states (S_{glass}), i.e., $S = S_{liquid} - S_{glass}$. In addition, we also follow Chow's assumptions [21] that configurational entropies of glass state are zero and ΔC_P , i.e., difference in heat capacity between the liquid and glass, is independent of temperature and composition, thus we can express the change in T_g when nanoparticles (X) are added by [19–21]:

$$\ln \left(\frac{T_g(X)}{T_g(X=0)} \right) = -\frac{1}{\Delta C_P} (S(X) - S(X=0)). \quad (1)$$

We assume that configurational entropies are composed by the disorientation entropies of polymer 1 (S_{dis-1}) and polymer 2 (S_{dis-2}), the mixing entropies (S_{mix-12} , S_{mix-1X} , S_{mix-2X}), the specific interaction entropies (S_{spe-12} , S_{spe-1X} , S_{spe-2X}) and the confinement entropies of the nanoparticles (S_{con-1X} , S_{con-2X}). The configurational entropies for $S(X)$ and $S(X=0)$ are given by:

$$S(X) = S_{dis-1} + S_{dis-2} + S_{mix-12} + S_{mix-1X} + S_{mix-2X} + S_{spe-12} + S_{spe-1X} + S_{spe-2X} + S_{con-1X} + S_{con-2X} \quad (2)$$

and

$$S(X=0) = S_{dis-1} + S_{dis-2} + S_{mix-12} + S_{spe-12}. \quad (3)$$

Then, by substituting these entropies in the above equation we obtain:

$$\ln \left(\frac{T_g(X)}{T_g(X=0)} \right) = -\frac{1}{\Delta C_P} (S_{mix-1X} + S_{mix-2X} + S_{spe-1X} + S_{spe-2X} + S_{con-1X} + S_{con-2X}). \quad (4)$$

The expressions that relate each type of single entropy are described in Table 1 [19]. In addition, we will assume: (a) The specific interaction between polymers and nanoparticles are related linearly with the crosslinker concentration ($\gamma_{spe-iX} = \gamma_{ia} + \gamma_{ib}C$), and (b) the volumetric fraction of nanoparticles is proportional to the mass fraction ($\phi_X \propto X$). Then, by substituting the terms in Table 1 and factoring, we obtain:

$$\ln \left(\frac{T_g(C, X)}{T_g(C, X=0)} \right) = \alpha_1 + \alpha_2 C + \beta_1 X \ln X + \beta_2 C X \ln X + \beta_3 X^2 + \alpha_3 X^3, \quad (5)$$

where α_j and β_j (with $j = 1, 2, 3$) are parameters obtained from regrouping other terms. By setting the boundary condition $\lim_{X \rightarrow 0} \ln \left(\frac{T_g(C, X)}{T_g(C, X=0)} \right) = 0$, we obtain that: $\alpha_1 + \alpha_2 C = 0$ ($\forall C$). In addition, in order to simplify the equation, the higher order term X^3 is disregarded ($0 \leq X < 1 \Rightarrow X^3 \ll 1$). With these considerations taken into account, we obtain a general expression for the change in the glass transition temperature:

$$\ln \left(\frac{T_g(C, X)}{T_g(C, X=0)} \right) = (\beta_1 + \beta_2 C) X \ln X + \beta_3 X^2, \quad (6)$$

where β_1 , β_2 and β_3 are parameters of the material that can be fitted to experimental data, or obtained if the molecular properties are known:

$$\beta_1 = \frac{k_B}{r_X \Delta C_P} \left(4 - (\gamma_{1a} + \gamma_{2a}) \ln \left(\frac{z-1}{e} \right) \right), \quad (7)$$

$$\beta_2 = -\frac{k_B}{r_X \Delta C_P} \left((\gamma_{1b} + \gamma_{2b}) \ln \left(\frac{z-1}{e} \right) \right), \quad (8)$$

$$\beta_3 = -\frac{4k_B}{r_X \Delta C_P} \left(\frac{\tanh\left(1 - \frac{R_X}{r_{0,1}}\right)}{\phi_1} + \frac{\tanh\left(1 - \frac{R_X}{r_{0,2}}\right)}{\phi_2} \right). \tag{9}$$

Table 1. Configurational entropies used in the theoretical modelling, where k_B is the Boltzmann constant, ϕ_i is the volume fraction of polymer i (with $i = 1, 2$), ϕ_X is the volume fraction of nanoparticles, r_i is the molar volume of polymer i , r_X is the molar volume of nanoparticles, R_X is the nanoparticle radius, $r_{0,i}$ is the average monomer radius of the polymer i , z is the lattice coordination number and γ_{spe-iX} is a parameter representing the specific interaction between the polymer i and nanoparticle.

| Configurational Entropy | Equation |
|--|--|
| Mixing entropy | $S_{mix-iX} = -k_B \left(\frac{\phi_i}{r_i} \ln \phi_i + \frac{\phi_X}{r_X} \ln \phi_X \right)$ |
| Specific interaction entropy | $S_{spe-iX} = \gamma_{spe-iX} k_B \ln \left(\frac{z-1}{e} \right) \left(\frac{\phi_i}{r_i} \ln \phi_i + \frac{\phi_X}{r_X} \ln \phi_X \right)$ |
| Confinement entropies of nanoparticles | $S_{con-iX} = -k_B \frac{\phi_X}{r_X} \left(\ln \phi_X + \tanh \left(\frac{R_X}{r_{0,i}} - 1 \right) \frac{4\phi_X - 3\phi_X^2}{\phi_i} \right)$ |

3.3. Experimental Application of the Model

We apply Equation (6) to our experimental glass transition measurements and obtain intrinsic scaffold parameters (β_i). The data obtained of the full factorial design 3^2 was used to contrast this model with experimental results (Figure 3).

Figure 3a displays a single set of fitting parameters for experimental information obtained previously. The obtained coefficient of determination was $R^2 = 0.999$. The experimental data is in good agreement with the proposed model. The intrinsic material parameters β_1 , β_2 and β_3 obtained from fitting the experimental data: $\beta_1 = -0.136$, $\beta_2 = 4.359 [\%^{-1}]$ and $\beta_3 = 1.506$.

Figure 3b shows the experimental data points together with the fitted surface obtained from the single set of fitted parameters: β_1 , β_2 and β_3 . The trends in the model show good agreement with the experimental results.

We also tested the model on other systems, where we have modified the original scaffolds with a 0.10% crosslinker concentration. One modification was to change the freezing temperature, i.e., the previous step to freeze-drying, from $-20\text{ }^\circ\text{C}$ to $-196\text{ }^\circ\text{C}$ by using liquid nitrogen. The other modification was to change the molecular weight (MW) of the chitosan used in the scaffold from 120 kDa to 300 kDa. Figure 4 shows that molecular weight has a smaller effect on the shape of the curve than the freezing temperature. Overall, the scaffolds fabricated exhibit a similar behaviour in T_g , first decreasing and then increasing as a function of nanoparticle mass fraction.

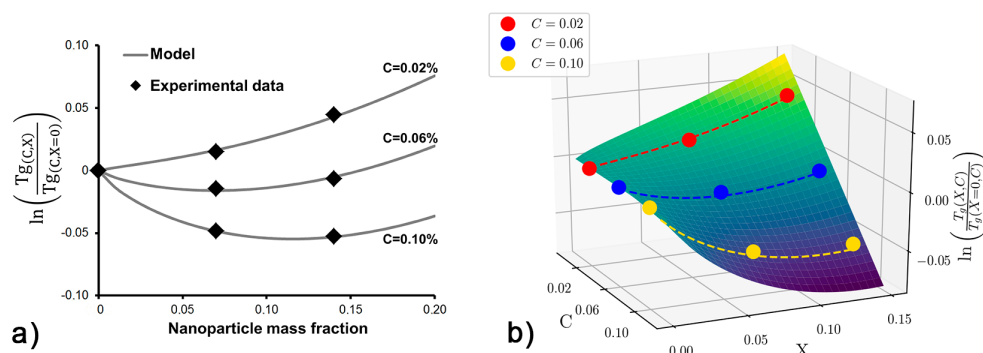


Figure 3. (a) Change in glass transition temperatures as a function of nanoparticles mass fraction for three different crosslinker concentrations. Solid lines represent our proposed model. (b) Reconstructed surface plot obtained using the fitted parameters (β_i) and experimental points (solid dots).

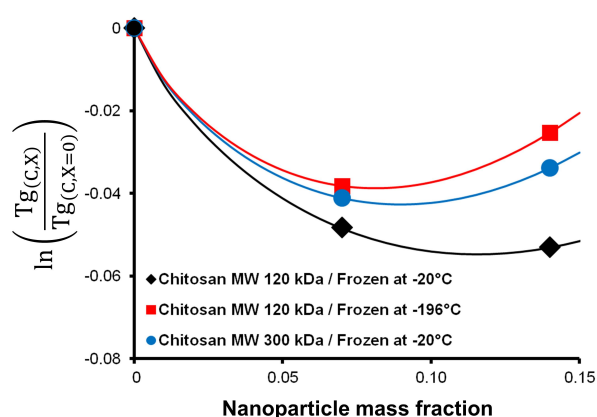


Figure 4. Application of the model to different systems using a fixed crosslinker concentration of 0.10%. Experimental data of the original scaffold (black diamonds), modification of the freezing temperature (red squares) and change of the chitosan molecular weight (blue dots) are shown.

Changes in T_g were mathematically modelled, and predicted values come to good agreement with the experimental behavior. We propose that this model can be used in the design of crosslinking processes used in the fabrication of nanocomposite scaffolds. This is a first approach and more experimental work is undoubtedly necessary to validate the equation with other nanocomposite scaffolds.

4. Conclusions

The glass transition temperature of a biopolymer scaffold changes when it is crosslinked or modified by nanoparticles addition. Our results suggest that there are synergic effects between nanoparticles and crosslinking, which lead to a non-linear behavior of the glass transition temperature. Moreover, a theoretical model to estimate the T_g was developed and fitted to experimental data. The model represents the experimental behavior of the glass transition and can be used as a mathematical tool for the design of scaffolds with specific physical properties, in particular T_g .

Author Contributions: conceptualization, T.P.C. and C.A.A.; experimental methodology, J.C.F. and C.A.A.; theoretical analysis, K.N.C., T.P.C. and C.P.R.; writing original draft preparation, K.N.C.; writing, review and editing, T.P.C., C.P.R. and C.A.A.; project administration, T.P.C. and C.A.A.

Funding: This research received no external funding.

Acknowledgments: K.N.C. acknowledges research funding from DGIIP-USM by PIIC Scholarship (K.N.C. 2017-2), C.A.A. acknowledges Conicyt by Basal Centre CCTVal FB0821 and T.P.C. acknowledges funding from Conicyt by Fondecyt Initiation 11160664.

Conflicts of Interest: The authors declare no conflict of interest.

References

- Smith, I.O.; Liu, X.H.; Smith, L.A.; Ma, P.X. Nanostructured polymer scaffolds for tissue engineering and regenerative medicine. *WIREs Nanomed. Nanobiotechnol.* **2009**, *1*, 226–236. [[CrossRef](#)] [[PubMed](#)]
- Paul, D.R.; Robeson, L.M. Polymer nanotechnology: Nanocomposites. *Polymer* **2008**, *49*, 3187–3204. [[CrossRef](#)]
- Ishii-Hyakutake, M.; Mizuno, S.; Tsuge, T. Biosynthesis and Characteristics of Aromatic Polyhydroxyalkanoates. *Polymers* **2018**, *10*, 1267. [[CrossRef](#)]
- Rittigstein, P.; Priestley, R.D.; Broadbelt, L.J.; Torkelson, J.M. Model polymer nanocomposites provide an understanding of confinement effects in real nanocomposites. *Nat. Mater.* **2007**, *6*, 278–282. [[CrossRef](#)] [[PubMed](#)]
- Acevedo, C.A.; Sánchez, E.; Díaz-Calderón, P.; Blaker, J.J.; Enrione, J.; Quero, F. Synergistic effects of crosslinking and chitosan molecular weight on the microstructure, molecular mobility, thermal and sorption properties of porous chitosan/gelatin/hyaluronic acid scaffolds. *J. Appl. Polym. Sci.* **2017**, *134*, 44772. [[CrossRef](#)]

6. Heath, D.E.; Cooper, S.L. Interaction of Endothelial Cells with Methacrylic Terpolymer Biomaterials. *J. Biomed. Mater. Res. B Appl. Biomater.* **2010**, *92*, 289–297. [[CrossRef](#)] [[PubMed](#)]
7. Heath, D.E.; Kobe, C.; Jones, D.; Moldovan, N.I.; Cooper, S.L. In Vitro Endothelialization of Electrospun Terpolymer Scaffolds: Evaluation of Scaffold Type and Cell Source. *Tissue Eng. Part A* **2013**, *19*, 79–90. [[CrossRef](#)] [[PubMed](#)]
8. Enrione, J.; Díaz, P.; Weinstein-Opppenheimer, C.; Sánchez, E.; Fuentes, M.A.; Brown, D.I.; Herrera, H.; Acevedo, C.A. Designing a gelatin/chitosan/hyaluronic acid biopolymer using a thermophysical approach for use in tissue engineering. *Bioprocess Biosyst. Eng.* **2013**, *36*, 1947–1956. [[CrossRef](#)]
9. Forero, J.C.; Roa, E.; Reyes, J.G.; Acevedo, C.; Osses, N. Development of Useful Biomaterial for Bone Tissue Engineering by Incorporating Nano-Copper-Zinc Alloy (nCuZn) in Chitosan/Gelatin/Nano-Hydroxyapatite (Ch/G/nHAp) Scaffold. *Materials* **2017**, *10*, 1177. [[CrossRef](#)]
10. Weinstein-Opppenheimer, C.R.; Brown, D.I.; Coloma, R.; Morales, P.; Reyna-Jeldes, M.; Díaz M.J.; Sánchez, E.; Acevedo, C.A. Design of a hybrid biomaterial for tissue engineering: Biopolymer-scaffold integrated with an autologous hydrogel carrying mesenchymal stem-cells. *Mater. Sci. Eng. C* **2017**, *79*, 821–830. [[CrossRef](#)] [[PubMed](#)]
11. Yoshioka, T.; Kawazoe, N.; Tateishi, T.; Chen, G. In vitro evaluation of biodegradation of poly(lactic-co-glycolic acid) sponges. *Biomaterials* **2008**, *29*, 3438–3443. [[CrossRef](#)] [[PubMed](#)]
12. Acevedo, C.A.; Somoza, R.A.; Weinstein-Opppenheimer, C.; Silva, S.; Moreno, M.; Sánchez, E.; Albornoz, F.; Young, M.E.; MacNaughtan, W.; Enrione, J. Improvement of human skin cell growth by radiation induced modifications of a Ge/Ch/Ha scaffold. *Bioprocess Biosyst. Eng.* **2013**, *36*, 317–324. [[CrossRef](#)]
13. Acevedo, C.A.; Díaz-Calderón, P.; Enrione, J.; Caneo, M.J.; Palacios, C.F.; Weinstein-Opppenheimer, C.; Brown, D.I. Improvement of biomaterials used in tissue engineering by an ageing treatment. *Bioprocess Biosyst. Eng.* **2015**, *38*, 777–785. [[CrossRef](#)]
14. Fox, T.G.; Flory, P.J. Second-Order Transition Temperatures and Related Properties of Polystyrene. I. Influence of Molecular Weight. *J. Appl. Phys.* **1950**, *21*, 581–591. [[CrossRef](#)]
15. White, R.P.; Lipson, J.E.G. Polymer free volume and its connection to the glass transition. *Macromolecules* **2016**, *49*, 3987–4007. [[CrossRef](#)]
16. Lipson, J.E.G.; Milner, S.T. Local and average glass transitions in polymer thin films. *Macromolecules* **2010**, *43*, 9874–9880. [[CrossRef](#)]
17. White, R.P.; Price, C.C.; Lipson, J.E.G. Effect of interfaces on the glass transition of supported and freestanding polymer thin films. *Macromolecules* **2015**, *48*, 4132–4141. [[CrossRef](#)]
18. Milner, S.T.; Lipson, J.E.G. Delayed glassification model for free-surface suppression of Tg in polymer glasses. *Macromolecules* **2010**, *43*, 9865–9873. [[CrossRef](#)]
19. Lee, K.J.; Lee, D.K.; Kim, Y.W.; Choe, W.; Kim, J.H. Theoretical consideration on the glass transition behavior of polymer nanocomposites. *J. Polym. Sci. B Polym. Phys.* **2007**, *45*, 2232–2238. [[CrossRef](#)]
20. Gibbs, J.H.; DiMarzio, E.A. Nature of the Glass Transition and the Glassy State. *J. Chem. Phys.* **1958**, *28*, 373–383. [[CrossRef](#)]
21. Chow, T.S. Molecular Interpretation of the Glass Transition Temperature of Polymer-Diluent Systems. *Macromolecules* **1980**, *13*, 362–364. [[CrossRef](#)]

